

Overannealing effects in GaInNAs(Sb) alloys and their importance to laser applications

Seth R. Bank,^{a)} Homan B. Yuen, Hopil Bae, Mark A. Wistey, and James S. Harris, Jr.
Solid State and Photonics Laboratory, Stanford University, Stanford, California 94305

(Received 18 November 2005; accepted 17 April 2006; published online 2 June 2006)

The photoluminescence efficiency and linewidth are well-established metrics for characterizing potential laser active regions. We demonstrate the critical importance of a new parameter for predicting the performance of dilute-nitride lasers: the “optimal” postgrowth annealing temperature, defined as the annealing temperature giving the highest photoluminescence efficiency. We validate this assertion with two 1.55 μm edge-emitting GaInNAsSb lasers containing active regions with different optimal annealing temperatures. Although both active regions showed comparable photoluminescence efficiency and linewidth under optimal annealing conditions, laser performance was significantly different. The room-temperature threshold current density for the active region with higher optimal annealing temperature was 630 A/cm², compared with 2380 A/cm² for the sample with lower optimal annealing temperature. We conclude that overannealing of the gain region during upper cladding growth is the responsible mechanism. The dependence of the optimal annealing temperature on composition and growth conditions is also discussed. © 2006 American Institute of Physics. [DOI: 10.1063/1.2208375]

The dilute-nitride system, GaInNAs, was originally proposed by Kondow *et al.* to produce temperature stable 1.3 μm lasers on GaAs substrates.¹ The GaAs substrate introduces additional advantages for long-wavelength vertical-cavity surface-emitting lasers (VCSELs), including high-quality native oxide layers for current and optical confinements and AlAs/GaAs distributed Bragg reflector mirrors. Despite the difficulties associated with GaInNAs growth, excellent 1.3 μm lasers have been demonstrated.^{2,3} Lasing has been successfully extended to 1.51 μm with thresholds of 780 A/cm² and even to 1.59 μm but with significantly degraded threshold.⁴ A promising method to improve material quality and laser performance is to add antimony, forming GaInNAsSb.^{5–9} Antimony reduces point defects, promotes two-dimensional growth, suppresses phase segregation via well known surfactant effects, and incorporates into the lattice to further redshift the emission. This allowed the first low-threshold continuous-wave lasers on GaAs emitting at 1.5 μm with pulsed thresholds as low as 440 A/cm².^{9,10} The subsequent Infineon GaInNAs result⁴ was followed shortly by the demonstration of GaInNAsSb lasers at 1.55 μm (Ref. 11) and later by others;¹² however, the target of low-threshold 1.55 μm lasers—and ultimately monolithic VCSELs—has remained elusive until now. We present low-threshold 1.55 μm lasers that were enabled by increasing the thermal robustness of the active region sufficiently to withstand the *in situ* annealing effects during the top cladding layer growth.

It is well known that the photoluminescence (PL) efficiency⁴ and linewidth¹³ are important metrics for gauging the quality of dilute-nitride active regions, due to their sensitivity to nonradiative centers and structural quality. However, another quantity is also critically important: the “optimal” annealing temperature. Thermal annealing of the dilute-nitride quantum well (QW), *in situ* and/or *ex situ*, is crucial

for obtaining high luminescence efficiency.^{14–16} To fully characterize the QWs and to gauge their optical quality, samples are typically cleaved into pieces and *ex situ* annealed at a range of times and/or temperatures. As shown in Fig. 1, PL efficiency increases at short times and/or low temperatures, followed by a precipitous decrease at longer times and/or higher temperatures. The optimal annealing point is a well-known phenomenon in the dilute nitrides and has been reported by several groups.^{15,17,18} Degradation of the optical quality at high annealing temperatures has been attributed to mechanisms ranging from the propagation of arsenic vacancies created at the sample surface during annealing^{17,19} to an *intrinsic* degradation of the metastable QW.¹⁸ Little, if any, attention has been paid to the significance of this parameter for device applications, however. We find that the optimal annealing temperature is an important property that measures the thermal budget of the active region and, consequently, how much material can be grown above the QW without degradation. We present two QW structures of slightly different compositions, both emitting at 1.55 μm with virtually identical luminescence efficiency and linewidth, but different

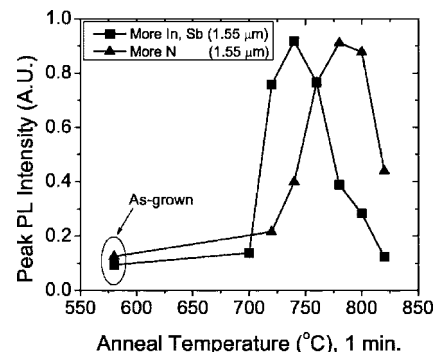


FIG. 1. Peak PL intensity, as a function of annealing temperature, for two QWs emitting $\sim 1.54 \mu\text{m}$ after optimal annealing. The optimal annealing temperature was significantly lower for the more highly strained QW containing more indium and antimony.

^{a)}Electronic mail: sbank@stanfordalumni.org

optimal annealing temperatures. The active region with a higher optimal annealing temperature produced substantially improved lasers. High-resolution x-ray diffraction (HRXRD) and PL were employed to corroborate the laser results and to study the nature of the degradation. In a related set of experiments, the optimal annealing temperature was found to decrease with increasing indium content, but was unaffected by the nitrogen mole fraction and the antimony flux. This indicates that strain is not the sole factor determining the thermal budget of the QW and that there is a chemical component. We note, in passing, that the optimal annealing temperature is also independent of the growth temperature and arsenic flux employed during active region growth.

Samples were grown by solid-source molecular beam epitaxy on (100) GaAs substrates with nitrogen supplied from a rf plasma cell and antimony from an unvalved cracking cell. GaInNAsSb and GaNAs layers were grown at 440 °C with a 20× and 15× As/group-III beam-equivalent–pressure ratio, respectively. *Ex situ* annealing was performed in a rapid thermal annealing furnace under flowing nitrogen gas. Arsenic desorption was minimized with a GaAs proximity cap. Samples with two different active regions were grown. The active region with lower optimal annealing temperature was a single 75 Å Ga_{0.59}In_{0.41}N_{0.028}As_{0.942}Sb_{0.03} QW (+2.64% strain) surrounded on either side by 210 Å GaN_{0.03}As_{0.97} strain-compensating barriers. The active region with a higher optimal annealing temperature was a single 75 Å Ga_{0.62}In_{0.38}N_{0.030}As_{0.943}Sb_{0.027} QW (+2.48% strain) surrounded on either side by 210 Å GaN_{0.04}As_{0.96} barriers. For PL structures, the active layer was grown on a 3000 Å GaAs buffer and capped with 500 Å of GaAs, both grown at 580 °C. Further details of the growth, including laser structure and device fabrication, are given elsewhere.^{9,10}

Figure 1 shows the postgrowth annealing behavior of the two active regions embedded in a PL structure. The optimal peak PL efficiencies were virtually identical, but occurred at significantly different annealing temperatures. Luminescence linewidths were also comparable, ~35 meV. The effects of overannealing in these samples were evident in (004) $\omega/2\theta$ HRXRD measurements. The most striking differences, when comparing overannealed material to as-grown and optimally annealed samples, were (a) the loss of QW-related Pendellösung fringes and (b) a decrease in the QW-related compressive strain—indicating significant structural degradation and loss of QW interface quality. No evidence of strain relaxation or phase segregation was observed with (224) reciprocal space mapping in overannealed material, however.

Room-temperature pulsed (1 μ s, 1% duty cycle) light output versus input current (*L-I*) curves for edge-emitting ridge-waveguide lasers based upon the two active regions are shown in Fig. 2. Lasing was centered at 1.552 and at 1.559 μ m for the QW with lower and higher optimal annealing temperatures, respectively. The devices were of similar size, but the laser with higher optimal annealing temperature showed significantly lower threshold current density, 630 vs 2380 A/cm², and higher external quantum efficiency, 44% vs 14%, than the laser with lower optimal anneal.²⁰ The differences are entirely due to *in situ* overannealing during the top cladding growth.

Studies of the effects of material growth above the QW validated that this source of *in situ* annealing can cause irreversible damage to the active layer. The active region was a

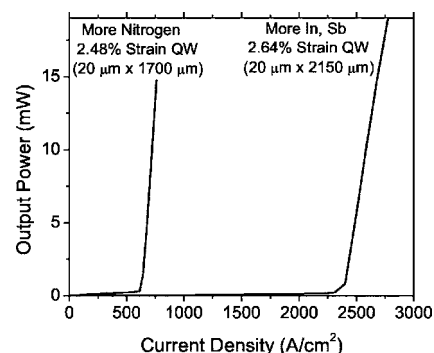


FIG. 2. Room-temperature pulsed *L-I* curves for lasers of similar dimensions based upon the two active regions of Fig. 1.²⁰

highly strained QW (+2.70%, 1.6 μ m emission) with a low optimal annealing temperature. For the first sample, a GaAs/Al_{0.33}Ga_{0.67}As waveguide, identical to that of the lasers (0.2 μ m GaAs, 1.8 μ m AlGaAs cladding, and 0.05 μ m GaAs cap), was grown above the QW at 560 °C. A second sample was grown with a somewhat thinner top cladding region (0.2 μ m GaAs, 1.1 μ m AlGaAs cladding, and 0.05 μ m GaAs cap), also at 560 °C. The *ex situ* annealing characteristics for the two structures are shown in Fig. 3. For the sample with a thicker top cladding, any subsequent annealing degraded the optical quality. The typical annealing-related behavior was recovered for the thinner 1.1 μ m cladding region. It is not fully understood why the optimal annealing temperature was ~800 °C—a significantly higher temperature than when embedded within a PL structure. This is likely due to the presence of multiple types of defects with differing activation energies for annealing. A long treatment at typical growth temperatures may remove one type of defect but has little effect on the other(s).²¹ As with PL efficiency and linewidth, it is important to compare the optimal annealing temperature between samples of identical structure. It is likely also beneficial to use PL test structures that reproduce the thermal cycling an active region experiences during device growth.

To determine whether the optimal annealing temperature is controlled simply by the strain or by a more complex mechanism, the QW nitrogen content was varied between 2.2% and 3.0%, with an active region consisting of a single 75 Å Ga_{0.62}In_{0.38}N_yAs_{0.973-y}Sb_{0.027} QW surrounded on either side by 210 Å GaN_zAs_{1-z} barriers and embedded in a PL structure. Samples emitted between 1.45 and 1.55 μ m after

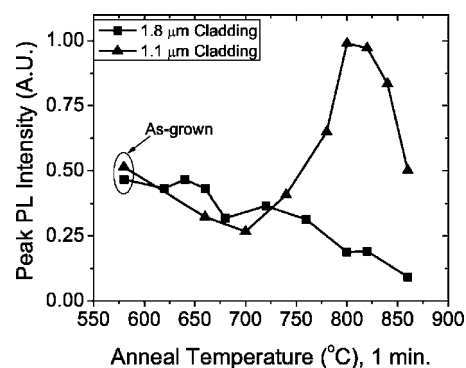


FIG. 3. *Ex situ* annealing behavior for nominally identical QWs subjected to different *in situ* annealings from the growth of different cladding thicknesses. The 1.8 μ m thick cladding overannealed the QW, but the typical annealing behavior was recovered with a thinner 1.1 μ m cladding.

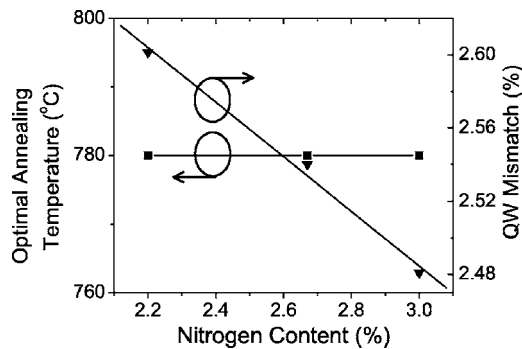


FIG. 4. Variation of the optimal annealing temperature for GaInNAsSb QWs, as a function of the nitrogen content. Also shown is the QW mismatch determined with HRXRD.

annealing, with comparable optical efficiency. The QW strain was varied from +2.48% to +2.60%, a range comparable to the difference in strain between the laser active regions of Figs. 1 and 2. As shown in Fig. 4, no difference was found in the optimal annealing temperature, indicating that strain is not the sole determining factor. These findings are consistent with those of Mussler *et al.* for GaNAs of similar nitrogen contents.¹⁸

In two additional, separate sets of experiments, the indium and antimony contents were also varied. The active region was a single 70 Å GaInNAs(Sb) QW, containing ~2% nitrogen, and surrounded by GaAs and emitted at ~1.25–1.35 μm after annealing. For one set of samples, the antimony flux was fixed at 1×10^{-7} torr and the indium content was varied from 8% to 32%. In the other set of samples, the indium content was fixed at 32% and the antimony flux was varied from 0 to 1×10^{-7} torr. Further details of this study are presented elsewhere.²² It should be noted that varying the antimony flux increased the strain from +1.73% to +1.92% while increasing the indium content modulated the strain more substantially from +0.70% to +1.92%. The optimal annealing temperatures are summarized in Fig. 5. Increasing the indium content dramatically reduced the optimal annealing temperature, while varying the antimony flux had no discernable effect. The dependence upon indium content is consistent with previous reports for GaInNAs of low nitrogen content.¹⁵ This preliminary work indicates that the optimal annealing temperature may be most sensitive to the

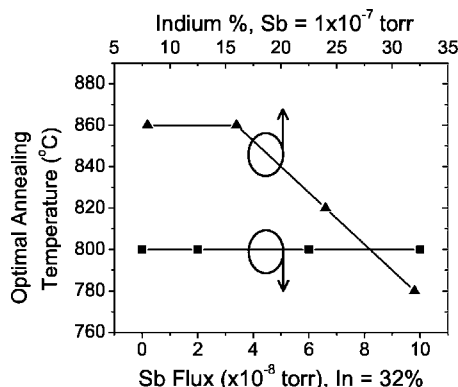


FIG. 5. Variation of the optimal annealing temperature for GaInNAsSb QWs, as functions of the indium content and antimony flux.

indium content; however, direct evidence and further study at higher indium mole fractions are certainly required.

The importance of the optimal annealing temperature to device design and growth has been proven and these findings have enabled low-threshold 1.55 μm lasers on GaAs. Further work is needed to identify the various mechanisms that determine the optimal annealing temperature; however, the effect is not purely due to strain. The optimal annealing temperature was found to be most sensitive to the indium content of the QW and independent of the nitrogen content. We also note, in passing, that the optimal annealing temperature is independent of the growth temperature and arsenic flux employed during active region growth. However, other growth parameters, such as the nitrogen plasma conditions, can have strong effects.

The authors thank T. Sarmiento and L. L. Goddard of Stanford University for many useful discussions and technical assistance, as well as Luxtron for the pyrometer used in this study. This work was supported by DARPA, ARO, the MARCO Interconnect Focus Center, and the Stanford Network Research Center (SNRC).

¹M. Kondow, K. Uomi, A. Niwa, T. Kitatani, S. Watahiki, and Y. Yazawa, *Jpn. J. Appl. Phys., Part 1* **35**, 1273 (1996).

²K. D. Choquette, J. F. Klem, A. J. Fischer, O. Blum, A. A. Allerman, I. J. Fritz, S. R. Kurtz, W. B. Breiland, R. Sieg, K. M. Geib, J. W. Scott, and R. L. Naone, *Electron. Lett.* **36**, 1388 (2000).

³N. Tansu and L. J. Mawst, *IEEE Photonics Technol. Lett.* **14**, 444 (2002).

⁴G. Jaschke, R. Averbeck, L. Geelhaar, and H. Riechert, *J. Cryst. Growth* **278**, 224 (2005).

⁵X. Yang, M. J. Jurkovic, J. B. Heroux, and W. I. Wang, *Appl. Phys. Lett.* **75**, 178 (1999).

⁶H. Shimizu, K. Kumada, S. Uchiyama, and A. Kasukawa, *Electron. Lett.* **36**, 1379 (2000).

⁷L. H. Li, V. Sallet, G. Patriarche, L. Largeau, S. Bouchoule, K. Merghem, L. Travers, and J. C. Harmand, *Electron. Lett.* **39**, 519 (2003).

⁸V. Gambin, W. Ha, M. A. Wistey, H. B. Yuen, S. R. Bank, S. M. Kim, and J. S. Harris, Jr., *IEEE J. Sel. Top. Quantum Electron.* **8**, 795 (2002).

⁹S. R. Bank, M. A. Wistey, H. B. Yuen, L. L. Goddard, W. Ha, and J. S. Harris, Jr., *IEEE J. Quantum Electron.* **40**, 656 (2004).

¹⁰S. R. Bank, M. A. Wistey, H. B. Yuen, L. L. Goddard, W. Ha, and J. S. Harris, Jr., *Electron. Lett.* **40**, 1186 (2004).

¹¹S. R. Bank, M. A. Wistey, H. B. Yuen, H. P. Bae, L. L. Goddard, and J. S. Harris, Jr., Spring 2005 MRS Meeting, San Francisco, CA, March 2005 (unpublished).

¹²J. A. Gupta, P. Barrios, X. Zhang, G. Pakulski, and X. Wu, 47th Electronic Materials Conference, Santa Barbara, CA, June 2005 (unpublished).

¹³M. Fischer, D. Gollub, M. Reinhardt, M. Kamp, and A. Forchel, *J. Cryst. Growth* **251**, 353 (2003).

¹⁴E. V. Rao, A. Ougazzaden, Y. Le Bellego, and M. Juhel, *Appl. Phys. Lett.* **72**, 1409 (1998).

¹⁵T. Kageyama, T. Miyamoto, S. Makino, F. Koyama, and K. Iga, *Jpn. J. Appl. Phys., Part 2* **38**, L298 (1999).

¹⁶H. P. Xin, K. L. Kavanagh, M. Kondow, and C. W. Tu, *J. Cryst. Growth* **201–202**, 419 (1999).

¹⁷S. Govindaraju, J. M. Reifsnider, M. M. Oye, and A. L. Holmes, Jr., *J. Electron. Mater.* **33**, 851 (2004).

¹⁸G. Mussler, J.-M. Chauveau, A. Trampert, M. Ramsteiner, L. Däweritz, and K. H. Ploog, *J. Cryst. Growth* **267**, 60 (2004).

¹⁹Sylvia G. Spruytte, Ph.D. thesis, Stanford University, 1999.

²⁰Cavity length studies verified that the difference in cavity lengths was insufficient to explain the improved external efficiency.

²¹J. S. Harris, J. W. Mayer, F. H. Eisen, J. D. Haskell, B. Welch, and R. D. Pashley, *Appl. Phys. Lett.* **21**, 601 (1972).

²²H. B. Yuen, S. R. Bank, H. P. Bae, M. A. Wistey, and J. S. Harris, *J. Appl. Phys.* **99**, 093504 (2006).